A predictive model for the peak shear strength of infilled soft rock joints developed with a multilayer perceptron

Ana Raquel Sena Leite[1,#] (ID), Silvrano Adonias Dantas Neto[1] (ID)

Article

Abstract

Several analytical methodologies help estimate the shear strength of rock discontinuities whose main limitations are the difficulty to obtain all necessary parameters to satisfactorily represent the boundary conditions and influence of infill materials. The objective of this study is to present a predictive model of peak shear strength for soft rock discontinuities developed making use of an artificial neural network known as multilayer perceptron. The model's input variables are: normal stiffness; initial normal stress acting on the discontinuity; joint roughness coefficient (JRC); ratio t/a (fill thickness/asperity height); uniaxial compressive strength and the basic friction angle of the intact rock; and finally the internal friction angle of infill material. To do so, results from 115 direct shear tests, with different soft rock discontinuities conditions were used. The herein proposed ANN predictive model, with an architecture 7-20-1, have shown coefficient of correlation in training and validation of 99.8 % and 99 %, respectively. The results from the model satisfactorily fit the experimental data and were also able to represent the influence of the input variables on the peak shear strength of soft rock discontinuities for different infill and boundary conditions.

1. Introduction

The peak shear strength is the leading mechanical property of interest when adopting limit equilibrium theories for design and analyze a project whose failure mechanisms are governed by the discontinuities existing in a rock mass. Consequently, it is of the utmost importance to determine it in order to develop rational designs in Rock Mechanics.

Several analytical formulations help estimate the shear strength of rock discontinuities, and it is worth mentioning traditional methods such Patton (1966), Barton (1973), Barton & Choubey (1977), Barton & Bandis (1982, 1990). In such methodologies, the shear strength of rock discontinuities is determined indirectly considering the discontinuities roughness, uniaxial compressive strength of the intact rock or wall strength, and the initial normal stress. These simplified models having been validated by direct shear tests performed under constant normal load conditions (CNL), for certain load conditions. However, parameters such as the presence of infill material and also normal

stiffness caused by the surrounding rock mass or rock bolts, which significantly influence the shear strength of the discontinuities are not considered (Ladanyi & Archambault, 1977; Papaliangas et al., 1993; Haque, 1999; Haque & Indraratna, 2000; Indraratna et al., 1999, 2005, 2010, 2012, 2013, 2014, 2015; Oliveira et al., 2009; Naghadehi, 2015; Karakus et al., 2016; Mehrishal et al., 2016; Shrivastava & Rao, 2017). On the other hand, the use of analytical models for rationally considering the effect of the infill and the normal stiffness of the rock discontinuities is hampered by the number of parameters required. These parameters obtained by direct shear tests are not always able to represent the discontinuity's boundary conditions satisfactorily and comprehensively (Ladanyi & Archambault, 1977; Papaliangas et al., 1993; Indraratna et al., 1999; Oliveira et al., 2009).

Nowadays, one of the increasingly used modelling techniques in geotechnical engineering to manage complex, multivariate and nonlinear phenomena are the artificial neural networks (ANN), especially those known as multilayer perceptrons (MLP). Many geotechnical applications have confirmed the efficiency of this tool in model-

#Corresponding author. E-mail address: ana.leite@ifce.edu.br.
[1]Departamento de Engenharia Hidráulica e Ambiental, Universidade Federal do Ceará, Fortaleza, CE, Brazil.

ling physical phenomena in geotechnics, such as, definition of longitudinal pavement defects (Farias et al., 2003), prediction of physical properties of asphalt materials for paving (Dantas Neto et al., 2004), development of models for estimating settlements in deep pile foundations (Amancio et al., 2014; Dantas Neto et al., 2014); predictive shear behavior in unfilled rock discontinuities (Dantas Neto et al., 2017).

Artificial neural networks are parallel processors massively distributed consisting of single processing units, which have a natural propensity to store experimental knowledge and make it available for use. From a mathematical viewpoint, an artificial neural network can be understood as a set of nodes, or neurons, organized in successive layers, analogous to the human brain. It has been proved useful in developing predictive models of complex, multivariate and nonlinear phenomena, as in the case of the shear strength of rock discontinuities. Among the benefits of making the use of artificial neural networks is the fact that, once their parameters are acquired, the predictive model can be easily implemented in any calculation spreadsheets, thereby facilitating their practical use in engineering.

This study proposes a predictive model for the peak shear strength of soft rock discontinuities by using a multilayer perceptron, a practical method that can be used in engineering daily basis without, in a first moment, the need of large-scale laboratory results, or even the use of hard-to-get parameters. The proposed predictive model presents as input variables the following: normal stiffness (k_n); the initial normal stress (σ_{no}) acting on the discontinuity; roughness of the discontinuity represented by the value of the joint roughness coefficient (JRC) proposed by Barton (1973); influence of the infill represented by the *t/a* ratio (thickness of the infill/asperity height); the characteristics of intact rock represented by uniaxial compressive strength (σ_c) and by the basic friction angle (ϕ_b); and at last the shear strength of the infill, if any, represented by its internal friction angle (ϕ').

2. Shear behavior of rock discontinuities

Peak shear strength of rock discontinuities is one of the critical mechanical properties used in Rock Mechanics design, mainly in situations that make use of limit equilibrium theories to analyze rock masses whose failure mechanisms are governed by such geological structures. There are several analytical methodologies to estimate the peak shear strength of rock discontinuities, the majority of them validated using results from large-scale direct shear tests performed under constant normal load conditions (CNL) and applicable only for cases of unfilled discontinuities.

Patton (1966), based on a series of large-scale direct shear tests under CNL conditions, proposed one of the first analytical models in Rock Mechanics to estimate the peak shear strength of unfilled rock discontinuities with regular roughness profiles. This author states that the failure enve-

lope of unfilled rock discontinuities presents a bilinear behavior represented by the curve B shown in Figure 1. It is observed that: for low levels of normal stress, the peak shear strength (τ_p) is given by sliding between the asperities, as a function of the applied normal stress (σ_n) and friction angle of the discontinuity, which is given by a combination of the basic friction angle (ϕ_r) of the rock and the roughness conditions of the discontinuity, represented by the angle of initial roughness inclination (i_o), as shown in Equation 1; while for high levels of normal load, the shearing occurs producing damage on the asperities, creating a cohesion intercept in the failure envelope given by Equation 2 after the sliding along a flat surface, with a friction angle equal to the basic or residual friction angle (ϕ_r).

Therefore, for low levels of normal stress, the shear strength of the discontinuities is given by the necessary friction to overcome the roughness caused by asperities and the rock-rock shear characterized by the basic friction angle. In contrast, for high load levels, the shear strength is the result og the effort required to produce the failure or degradation of the actual rough edges. Although it is quite a simple model, Patton's (1966) concept was the basis for numerous analytical methodologies, such as, the proposals by Indraratna et al. (2005, 2008a, b, 2013, 2014), Oliveira et al. (2009), Premadasa & Indraratna (2015), Shrivastava & Rao (2017).

$$\tau_p = \sigma_n \tan(\phi_b + i_o) \tag{1}$$

$$\tau_p = c_j + \sigma_n \tan \phi_b \tag{2}$$

Barton & Choubey (1977) proposed a predictive analytical model for the peak shear strength in unfilled discontinuities considering simultaneously the sliding between the asperities and their shearing represented in the bilinear envelope proposed by Patton (1966). In this, the peak shear strength can be estimated from the roughness of the discontinuity represented by the joint roughness coefficient (JRC), the joint compressive strength (JCS), obtained directly from the discontinuity wall using the Schmidt ham-
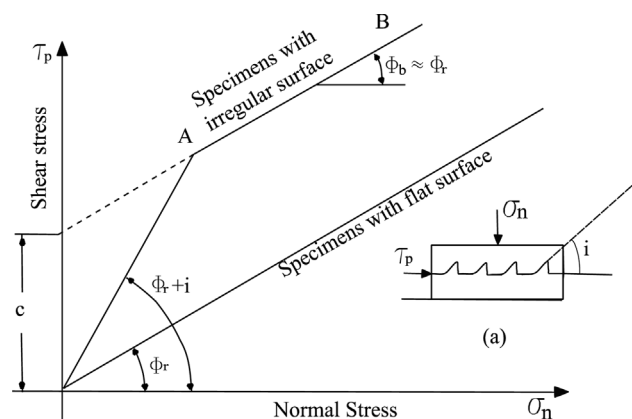

Figure 1. Shear strength envelope proposed by Patton (1966).

mer, and the residual friction angle (ϕ_r), as shown in Equation 3.

$$\tau_p = \sigma_n \tan\left[\text{JRC} \log\left(\frac{\text{JCS}}{\sigma_n}\right) + \phi_r \right] \qquad (3)$$

The residual friction angle presented in Equation 3 is estimated as a function of the basic friction angle of the rock (ϕ_b) and of the results of the Schmidt hammer tests as demonstrated in Equation 4.

$$\phi_r = (\phi_b - 20°) + 20\frac{r}{R} \qquad (4)$$

where R is the result from the sclerometer test in dry unweathered discontinuities, r is the result from the sclerometer test in wet weathered discontinuities.

Singh & Basu (2018) used results from 196 direct shear tests under CNL conditions to evaluate different analytical models for predicting the peak shear strength in unfilled rock discontinuities. This assessment was made using parameters such as the mean error and the root mean square error between the test results and the predictions from some existing models, obtaining the exposed in Table 1. According to these authors, although the models of Barton (1973) and Barton & Choubey (1977) are some of the most commonly used in Rock Mechanics, the models by Zhang et al., 2016, Yang et al. (2016) and Lee et al. (2014) provided results that are closer to the tests data than those obtained by applying the Barton (1973) and Barton & Choubey (1977) models.

The models by Xia et al. (2014), Zhang et al. (2016), and Yang et al. (2016) use the roughness characteristics of the discontinuities obtained by scanning the rock surface for the peak shear strength estimation, thus considering their three-dimensional morphology. However, having been considered an efficient representation when compared with other models by Singh & Basu (2018), obtaining the necessary parameters is somewhat difficult, considering the methodologies of classification and collecting data originally used in Rock Mechanics.

Studies by Horn & Deere (1962), Goodman (1969), Zeigler et al. (1972), Richard (1975), Ladanyi & Archambault (1977), Papaliangas et al. (1993), Haque (1999), Haque & Indraratna (2000), Indraratna et al. (1999, 2005, 2008a, b, 2010, 2012, 2013, 2014, 2015), Naghadehi (2015), Karakus et al. (2016), Mehrishal et al. (2016) and Shrivastava & Rao (2017), based on large-scale direct shear test results, demonstrate that other parameters not considered in the classical models presented on Equations 1 and 3 are also important when determining the shear strength of the rock discontinuities. Among which mention should be made of the following: the condition of normal stiffness of the discontinuity due the boundary conditions of the surrounding rock mass; type and strength characteristics of the infill material in the rock discontinuities; and the ratio between the infill thickness (t) and average height of the asperities (a), referred to as the t/a ratio.

Papaliangas et al. (1990) studied the shear strength of discontinuities filled with fine particles by carrying out direct shear tests on artificially shaped sandstone rock discontinuities with different JRC values (Figure 2). The authors' results showed a drop in the peak shear strength of
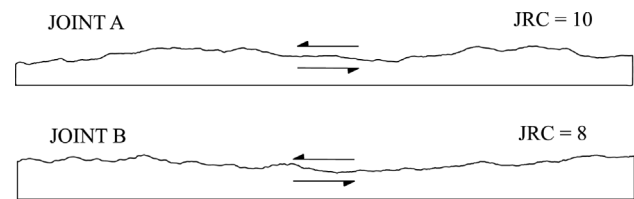

Figure 2. Discontinuity profiles tested by Papaliangas et al. (1990).

Table 1. Comparison between analytical methods for predicting the peak shear strength in rock discontinuities (Singh & Basu, 2018).

Shear strength criteria	Granite		Quartzite		Sandstone	
	Avg. error (%)	RMSE	Avg. error (%)	RMSE	Avg. error (%)	RMSE
Barton (1973)	12.17	0.102	26.68	0.198	20.57	0.185
Aydan et al. (1996)	21.06	0.188	20.12	0.175	31.93	0.304
Tatone & Grasselli (2009)	67.22	0.567	39.23	0.352	55.57	0.41
Gahzvinian et al. (2012)	55.07	0.448	30.82	0.262	44.19	0.307
Lee et al. (2014)	16.8	0.118	15.7	0.132	13.82	0.129
Tang et al. (2014)	27.45	0.224	13.87	0.102	12.16	0.096
Xia et al. (2014)	17.8	0.152	15.05	0.109	10.09	0.087
Jang & Jang (2015)	102.43	0.774	81.72	0.649	192.68	1.444
Kumar & Verma (2016)	22.05	0.241	19.54	0.136	18.57	0.181
Yang et al. (2016)	10.48	0.092	18.37	0.132	11.63	0.11
Zhang et al. (2016)	11.07	0.085	21.85	0.155	14.14	0.12

the rock discontinuities with the increase of the t/a ratio up to a critical value between 1.25 and 1.5. From this critical value of t/a, the shear strength of the rock discontinuity tends to remain constant, its strength becomes controlled only by the infill material.

Based on large-scale direct shear test results performed on infilled rock discontinuities under CNL, Papaliangas et al. (1993) proposed a model to estimate the friction coefficient (μ) of the discontinuity that considers the effect of the infill as seen in Equation 5 and Figure 3. In this equation, c and m are experimental constants, where c represents the critical t/a ratio and m the rate of shear strength reduction with the increase of infilling thickness. The authors recommend the following values: $c = 1$ for clayey infills and $c = 1.5$ for granular materials.

$$\mu = \mu_{min} + (\mu_{max} - \mu_{min})^{[1-\frac{1}{c}(\frac{t}{a})]^{m}} \tag{5}$$

Indraratna et al. (1999), in their experimental study, found that the influence of infill on the peak shear strength of saw-tooth soft rock discontinuities tested under CNL (constant normal load) and CNS (constant normal stiffness) conditions were similar. Those authors noted that there was a sharp drop in dilation during the shearing when the infill began to influence the failure mechanism of the rock discontinuities and proposed an hyperbolic equation to determine the drop in shear strength of the infilled discontinuities with the rise of the t/a ratio as shown in Equation 6.

$$\tau_{p,infilled} = \tau_{p,unfilled} - \sigma_{no} \frac{\frac{t}{a}}{\alpha(\frac{t}{a}) + \beta} \tag{6}$$

where $\tau_{p,infilled}$ is the peak shear strength of infilled discontinuity, $\tau_{p,unfilled}$ is the peak shear strength of unfilled discontinuity, σ_{no} is the initial normal stress acting on the rock discontinuity, α and β are empirical parameters.

Haque (1999) also proposed that the peak shear strength could be expressed by a Fourier series, as shown in Equation 7, with parameters regarding also the boundary conditions acting on the discontinuity, expressed by the initial normal stress (σ_{no}), normal stiffness (k_n), t/a ratio, basic
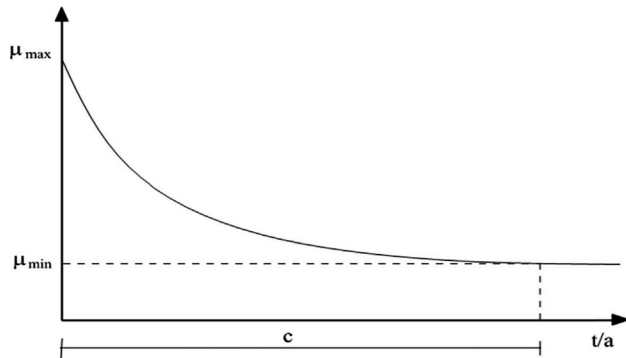

Figure 3. Variation of friction coefficient μ with the t/a ratio (Papaliangas et al., 1993).

friction angle (ϕ_b), and initial asperity angle (i_o). In Equation 7, h_p and i_{hp} are the horizontal displacement and dilation angle corresponding to the peak shear stress. The a_0, a_1 and T are the Fourier series parameters obtained by interpolating the experimental data from large-scale direct shear tests.

$$\tau_{p,infilled} = \left[\sigma_{no} + \frac{k_n}{A}\left(\frac{a_0}{2} + a_1 \cos\frac{2\pi h_p}{T}\right)\right] \times$$
$$\left[\frac{\tan\phi_b - \tan i_o}{1 - \tan\phi_b - \tan i_{hp}}\right] - \sigma_{no}\frac{\frac{t}{a}}{\alpha(\frac{t}{a}) + \beta} \tag{7}$$

Oliveira et al. (2009) developed the model shown in Equation 8 to predict the peak shear strength from direct shear tests under CNS conditions in saw-tooth rock discontinuities. In such a proposal, the authors considered the cohesion (c_{fill}) and friction angle (ϕ_{fill}) of infill material, and the $(t/a)_{cr}$ ratio in the estimation of peak shear strength, the dilatation angle at peak shear stress for clean joint ($i_{\tau p(clean)}$) and when compared to that one proposed by Haque (1999) and shown in Equation 7.

$$\tau_{p,infilled} = c'_{fill} + \sigma_n\left[\frac{\tan\phi_b + \tan i_0}{1 - \tan\phi_b - \tan i_{\tau p(clean)}}\right] \times$$
$$\left(1 - \frac{\frac{t}{a}}{(\frac{t}{a})_{cr}}\right)^{\alpha} + \tan\phi_{fill}\left(\frac{2}{1 + \frac{(\frac{t}{a})_{cr}}{\frac{t}{a}}}\right)^{\beta} \tag{8}$$

Shrivastava & Rao (2017) proposed a model to obtain the peak shear strength of infilled rock discontinuities after direct shear testing on saw-tooth rock discontinuities under CNL and CNS conditions, for different values of the t/a ratio, whose infill material was formed by fine sand and mica powder, and different roughness conditions. The model proposed by these authors uses the basic friction angle (ϕ_b) and the uniaxial compressive strength (σ_c) of the intact rock, the initial normal stress (σ_{no}) acting on the discontinuity, and the roughness of the discontinuity represented by the angle of its asperities (i), as shown in Equation 9. According to the authors, the parameter a can be close to the unit value ($a = 1$), and the value of b ranges from zero to 0.36, while constants x and y are obtained according to the conditions presented in Table 2.

$$\tau_p = (a\sigma_n + b)\tan\left[\phi_b + x\ln\left(\frac{a\sigma_n + b}{\sigma_c} + y\right)i\right] \tag{9}$$

Studies seeking to include the effect of infill material conditions (overconsolidation, unsaturation, water flow) in its shear strength were also implemented (Indraratna et al., 2008a, b, 2013, 2014; Premadasa & Indraratna, 2015). Such studies have shown that the evaluation of the influence of the various parameters on the peak shear strength of

Table 2. Coefficients *x* and *y* for different *t/a* values for be used in Equation 9.

i	*t/a*	*x*	*y*	R^2
30°-30°	0	-0.3	-0.356	0.95
	1	-0.26	-0.494	0.96
	1.4	-0.33	-0.821	0.99
	2	-0.13	-0.906	0.75
15°-15°	1	-0.51	-1.14	0.88
0°-0°	*t* = 5 mm	-0.07	0.73	0.99

the discontinuities has contributed to propose analytical models that satisfactorily represent this property for the widest variety of rock discontinuities and boundary conditions. However, the use of such analytical methodologies is still somewhat laborious, bearing in mind the need in specific cases to perform detailed laboratory tests to obtain the parameters required.

In order simplify the predictive process of the shearing behavior of discontinuities, eliminating many existing problems in the use of the current analytical proposals, it is worth mentioning some predictive models developed with artificial neural networks (ANN), fuzzy logic and neuro-fuzzy techniques, for instance the proposals by Dantas Neto et al. (2017), Matos (2018), and Matos et al. (2019a, b). Such models do not intend to replace other models or tests, but they present themselves as tools that can be used for estimating dilation and shear stress data of rock discontinuities enabling fast applications compatible with the day-to-day demands in engineering. Despite the good results presented by these models, they did not consider the infill materials which was the motivation for the present study.

3. Artificial neural networks

3.1 Basic concepts

Nowadays Artificial Neural Networks (ANN) are the computer models most commonly used in different areas of knowledge (Schmidhuber, 2015). ANN are based on the functioning of the human brain and its capacity to perceive and learn complex, nonlinear and multivariate phenomena (Dantas Neto et al., 2017; Chen et al., 2018; Schmidhuber, 2015).

Among the different kinds of existing artificial neural networks with well-proven applications in engineering, it is worth mentioning the multilayer perceptron (Dantas Neto et al., 2014, 2017; Schmidhuber, 2015; Haykin, 2008). The multilayer perceptron (MLP), illustrated in Figure 4, is a neural feedforward network comprising three types of layers: the input layer, consisting of nodes designed to receive stimulus from outside the system, that is, the values of the variables governing the modelled phenomenon; one or more hidden layers of neurons, responsible for increasing the capacity of the artificial neural network in extracting the most complex behavior or the environment in which it intends to establish a predictive model; and the output layer, comprising neurons whose signals are responses to the stimulus presented to the neural network.

Figure 5 shows the structure of each constituent artificial neuron of a multilayer perceptron, whose response in mathematical terms is obtained by successively applying Equation 10 to 12 (Haykin, 2008).

$$u_k = \sum w_{km} x_m = \{w\}^T \{x\} \tag{10}$$

$$v_k = u_k + b_k = \{w\}^T \{x\} + b_k \tag{11}$$

$$y_k = f(v_k) = f(\{w\}^T \{x\} + b_k) \tag{12}$$

where x_m are input variables, w_{km} are synaptic weights, v_k is the induced local field, u_k is the output of linear combiner, b_k is the bias, v_k is the induced local function, yk is the neuron output result, d_k are the expected result, ek is the output neuron error.

One of the most relevant properties of a neural network is its skill to learn from the environment in which it is inserted and to improve its performance through an ongoing training process. Training an artificial neural network consists of altering all synaptic weights (w_{kj}) and existing
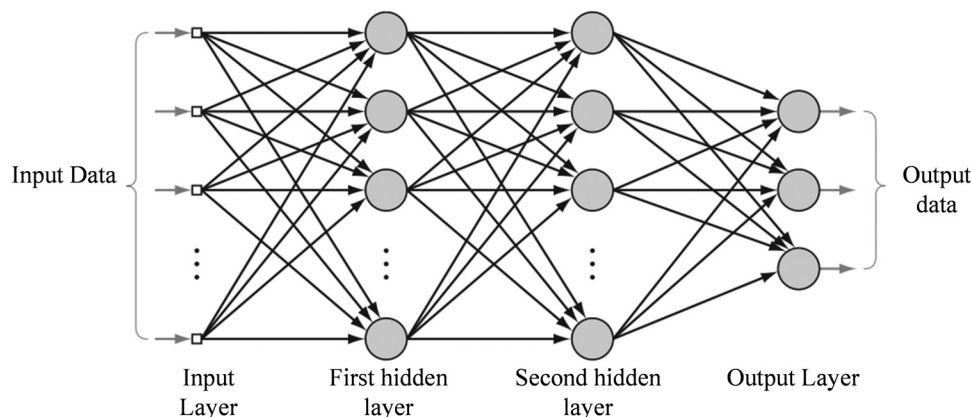

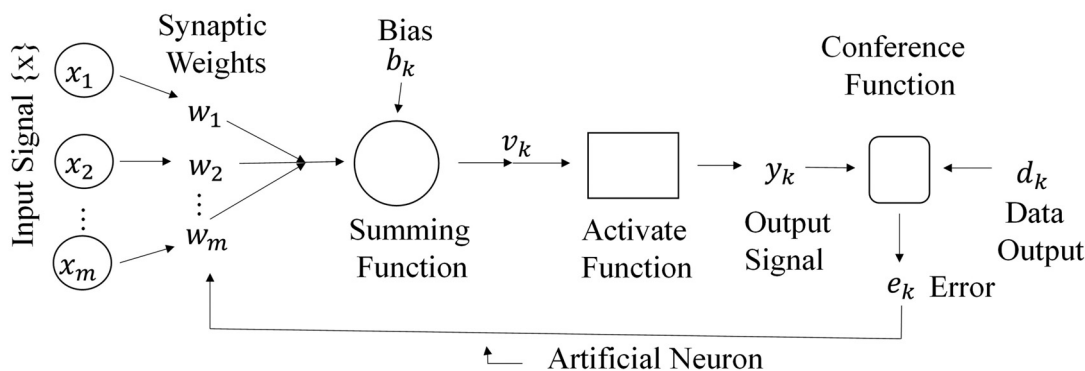**Figure 4.** Diagram of a multilayer perceptron (Haykin, 2008).

Figure 5. Diagram of an artificial neuron.

bias (b_k), from the known experience of the phenomenon studied, commonly available in a set of known in-out experimental data.

The performance of a neural network can be assessed by comparing the values obtaining for each neuron existing in the output layer with its corresponding one available in the training set, based on an average cost function defined as:

$$E_{med}(n) = \frac{1}{2L}\sum_{i=1}^{L}\sum_{kec} e_k^2 = \frac{1}{2L}\sum_{i=1}^{L}\sum_{kec}[d_k(i) - y_k(i)]^2 \quad (13)$$

where c is the set of all neurons from the output layer in the example I of the training set, $d_k(i)$ is the desired (known) output for the neuron k, in example i, $y_k(i)$ is the response calculated by neuron k, for the stimuli known in example i, $e_k(i)$ is the error signal of neuron k, in example i, n is the discrete period (period), corresponding to each alteration in the set of synaptic weights in the training set.

The training process of a neural network consists of successive adjustments of its synaptic weight to minimize the value of the average cost function throughout the available training set. For one neuron belonging to the output layer $y_k(n)$, the vector of the synaptic weights linking to the neurons of the previous layer $\{y_j(i)\}$ is adjusted by interactively minimizing the average cost function passing throughout the training set. This rule for altering the synaptic weights, known as Delta Rule, is described by the following expression:

$$w_{kj}(n+1) = w_{kj}(n) - \eta \nabla E_{med}(n)$$
$$= w_{kj}(n) + \frac{\eta}{L}\sum_{i=1}\delta_k(i)y_k(i) \quad (14)$$

where $w_{kj}(n+1)$ is the vector of synaptic weights between neurons k and j in the iteration (period) $n+1$, $w_{kj}(n)$ is the vector of synaptic weights between neurons k and j in the iteration n, $\nabla E_{med}(n)$ is the gradient of the average cost function, η is the learning rate, $y_j(i)$ is the vector of neuron input

$y_k(n)$ in the nth example available in the training set, $\delta_k(i)$ is the local gradient of neuron $y_k(n)$, defined as:

$$\delta_k(i) = e_k(i)f'(v_k(i)) \quad (15)$$

where $e_k(i)$ is the error signal of neuron $y_k(i)$ in the nth example of the training set, $v_k(i)$ is the induced local field of neuron $y_k(i)$ in the nth example of the training set.

For a neuron in the hidden layer, the direct calculation of the local gradient, according to Equation 15 is not possible, since the signal produced therein cannot be compared to a known value and, therefore, no error signal can be generated. In this case, the local gradient of the neuron in the hidden layer is determined by back-propagation of the error signal produced in the neurons in the output layer $y_k(i)$. This procedure is known as error backpropagation algorithm and was developed by Rumelhart et al. (1986), based on which the local gradient of a neuron belonging to a hidden layer immediately before the output layer is defined as:

$$\delta_j(i) = -\frac{1}{L}f'(v_j(i))\sum_i\sum_{k\in C}\delta_k(i)w_{kj}(n) \quad (16)$$

Bearing in mind the heavy dependence of the backpropagation algorithm convergence on the value of the learning rate adopted, Rumelhart et al. (1986) also proposed to introduce a parameter α, known as constant of momentum, in Equation 14 in order to improve the stability of the algorithm convergence resulting in the expression presented by Equation 17.

$$w_{kj}(n+1) = w_{kj}(n) + \frac{\eta}{L}\sum_{i=1}\delta_k(i)y_k(i) + \alpha(\Delta w_{kj}(n-1)) \quad (17)$$

3.2 Applications of the artificial neural networks in Rock Mechanics

In Rock Mechanics many studies were performed using neural networks as a powerful and valuable tool for developing predictive models. The majority of them contemplate the prediction of intact rock properties such as the uniaxial compressive strength (Grima et al., 2000; Mosh-

refii et al., 2018), Young's modulus (Sonmez et al., 2016; Yilmaz & Yusek, 2008; Dehghan et al., 2010), and even tensile strength (Singh et al., 2001). Concerning the development of predictive models for rock discontinuities using MLP, it is worth mentioning the studies by Dantas Neto et al. (2017) and Leite et al. (2019).

Dantas Neto et al. (2017) proposed a model of six input variables (normal stiffness, initial normal stress, JRC, uniaxial compressive strength of intact rock, basic friction angle and shear displacement), a hidden layer with 20 neurons, with the shear stress and dilation as the network outputs. This model was based on 44 direct shear tests obtained from the studies by Benmokrane & Ballivy (1989), Skinas et al. (1990), Papaliangas et al. (1993), Haque & Indraratna (2000), and Indraratna et al. (2010) and provided coefficients of correlation of 0.99 in both the training and testing phases. Although the results from the model satisfactorily fit the test results used in its development and can also satisfactorily express the influence of the input variables in the shear strength and dilation, this model is also to unfilled discontinuities.

Dantas Neto et al. (2018) provided an ANN predictive model of the shear strength of the unfilled discontinuities only for soft rock, considering as input variables normal stiffness (k_n), initial normal stress (σ_{no}), height (a) and initial inclination (i_o) of joint asperities and shear displacement (h) imposed on the discontinuity. The correlation coefficients were also high, approximately 0.99, both in the training and testing phases. This model's main limitations lie in the fact that the impact of the infill on the shear strength is not considered.

Leite et al. (2019) proposed a predictive model similar to the model suggested by Dantas Neto et al. (2017) but including the influence of the infill on the shear behavior of

the rock discontinuities. This neuronal model has an A:8-20-10-5-2 architecture, with eight (8) input neurons and three (3) hidden neuron layers, providing as output the shear stress and dilation of the rock discontinuity as a function of shear displacement imposed on the discontinuity. Correlation coefficients of 0.99 were obtained in both the training and validation phases of the model, which showed proper adjustments to the test data used in developing the model. This work was still preliminary with no further applicable information provided about the ANN model used and required a horizontal displacement data for its application.

4. Development of model

4.1 Data collection and definition of input variables

The present predictive model was developed based on the results of 115 direct shear tests performed by Haque & Indraratna (2000), Haque (1999), Indraratna et al. (2010), Oliveira et al. (2009), and Shrivastava & Rao (2017) on soft rock discontinuities with different characteristics and boundary conditions. The parameters used are listed below in Table 3. From the tests, 58 % were performed on infilled discontinuities and 67 % carried out under CNS conditions.

Based on the literature review, it is undeniable that the peak shear strength of the rock discontinuities is governed by its boundary conditions, roughness characteristics, intact rock properties and by the condition and shear strength characteristics of infill materials. Consequently, the following parameters were adopted as input variables for the predictive ANN model for the peak shear strength of soft rock discontinuities:

- x_1 = normal stiffness of the discontinuity (k_n), in kPa/mm;
- x_2 = t/a ratio;

Table 3. Joint parameters used in the ANN development.

Reference	Data	Joint type	Filling material	Limit	Normal stiffness (kPa/mm)	t/a	σ_{n0} (MPa)	JRC	σ_c (MPa)	ϕ_b (°)	ϕ_{fill} (°)	τ_p (MPa)
Indraratna & Haque (2000) and Haque (1999)	62	Saw-toothed	Bentonite	Min	0	0	0.16	2	12	32	0	0.14
				Max	453	1.8	2.69	13	20	37.5	35.5	3.34
Papaliangas et al. (1993)	11	Natural	Granular material	Min	0	0	0.05	12	3.5	30	0	0.02
				Max	0	1.1	0.1	12	3.5	30	30	0.1
Oliveira (2009) and Indraratna et al. (2010)	5	Saw-toothed	Clayey sand	Min	453	0	0.8	8	21.5	35.5	0	0.38
				Max	453	2	0.8	8	21.5	35.5	27.5	1.63
Shrivastava & Rao (2017)	37	Saw-toothed	Fine sand and mica dust	Min	0	0	0.05	7	11.75	30	0	0.08
				Max	90.7	2	2.04	15	11.75	30	28.8	2.6

- x_3 = initial normal stress (σ_{no}) acting on the discontinuity, in MPa;
- x_4 = JRC;
- x_5 = uniaxial compressive strength of intact rock (σ_c), in MPa;
- x_6 = basic friction angle (ϕ_b), in degrees;
- x_7 = internal friction angle of the discontinuity infill material (ϕ_{fill}), in degrees.

Although in the different studies that used experimental data to develop the model, the uniaxial compressive strength had been obtained from uniaxial compressive tests, in this study it is recommended that the σ_c value to be used for representing the uniaxial compressive strength of the intact rock be obtained from the Schmidt hammer. As a result, it shall take into account the change in intact rock properties, due to weathering action, in the determination of the rock discontinuities peak shear strength.

The expression in Equation 18 broadly represents the predictive model of the peak shear strength of soft rock discontinuities depending on their governing variables. The relationship between input and output variables of the neuronal model are defined by the neural network architecture, activation functions of its neurons and the values obtained for the synaptic weights and bias.

$$\tau_p = f\left(k_n, \frac{t}{a}, \sigma_{no}, \text{JRC}, \sigma_c, \phi_b, \phi_{fill}\right) \tag{18}$$

4.2 Training, testing and validation of the neuronal model

In order to set up the predictive neuronal model of the peak shear strength of soft rock discontinuities, eight (8) different architectures (7-30-1; 7-20-1; 7-15-1; 7-10-1; 7-30-15-1; 7-20-10-1; 7-30-15-5-1; 7-20-10-5-1) were used and submitted to the training, testing and validation phases

Training each ANN model represented by specific architecture consists of altering the synaptic weights using the backpropagation algorithm of Rumelhart et al. (1986) and the experimental data available in the training set formed by 80 %, randomly selected, of the 115 results of the aforementioned direct shear tests. During the training phase, the performance of each neuronal model studied was assessed from the variation in the number of iterations vs. the coefficient of correlation between the value of the output supplied by the neuronal model and the existing target-value in the training set for each used input-output example. In this study, the alterations in the synaptic

weights occurred up to a maximum of 1,000,000 iterations.

Test phase used the remaining 20 % of input-output examples in the available experimental data set that were left unused in the neuronal model training phase to assess the performance of the models when predicting data to which they were not submitted during the training phase. In addition to assessing the models' performance, monitoring the correlation values with the number of iterations in the test phase, also helps identify the optimal stopping point aiming to prevent any overfitting process that tends to impair the generalization capacity of the neuronal models (Haykin, 2008).

Validation phase consisted of assessing the neuronal models for the different architectures previously described by comparing the models' results with the test results. This enabled the identification of which models have enough capacity to properly interpolate the test results and satisfactorily express the influence of the different input variables in the peak shear strength of soft rock discontinuities.

The feedforward multilayer perceptron with backpropagation software QNET2000 was used in the training, testing and validation phases of the studied neuronal models. The sigmoid function given in Equation 19 was adopted to activate all neurons in the neuronal models studied because it is one of the most commonly used activation functions with satisfactory results in developing multilayer perceptron neuronal models (Runxuan, 2006; Dantas Neto et al., 2017, and Moshrefii et al., 2018).

$$f(x) = \frac{1}{1 + e^{-x}} \tag{19}$$

To calculate the error signals between the values available in the training set and those calculated by the studied neuronal models using the sigmoid function for activating the neurons in the output layer, it was necessary to normalize the input and output data available in the training and testing sets. This study involves normalizing these data in the 0.15 to 0.85 interval according to the Equation 20. Table 4 provides the variation intervals for the input and output variable values existing in the experimental set used for training and testing the studied neuronal models.

$$\frac{x_{nor} - 0.15}{0.85 - 0.15} = \frac{x - x_{min}}{x_{max} - x_{min}} \tag{20}$$

Table 4. Maximum and minimum values used for ANN training and validation.

k_n (kN/mm)	t/a	σ_{no} (MPa)	JRC	σ_c (MPa)	ϕ_b (°)	ϕ_{fill} (°)	τ_p (kPa)
0	0	0.05	2	3.5	30	21	20.8
453	2	2.69	15	21.5	37.5	35.5	3343

where x_{nor} is the normalized variable value, x_{min} is the minimum variable value in the training set, x_{max} is the maximum variable value in the training set.

In order to optimize the training process and, when altering the synaptic weights, avoid affecting any minimal points of the cost function, a variation range was used for the learning rate (η) of 0.001 and 0.1, and adopted the 0.8 value for the constant of momentum (α).

The criteria to define the best performing neuronal model to predict the peak shear strength of the soft rock discontinuities took into account the following aspects in order of priority: highest correlation value between the values available in the experimental set adopted and those calculated by the neural network in the test phase; the model's capacity to interpolate test data; and the model's capacity to represent the influence of input variables on the peak shear strength of soft rock discontinuities; and, in case of similarity for the above criteria, the model formed by the architecture with the smallest number of synaptic weights will be adopted.

5. Results and discussions

5.1 Training, testing and defining the model

Within the eight architectures studied in the search for a predictive neuronal model for the peak shear strength of soft rock discontinuities, the one with architecture 7-20-1 had the best performance since it provided in both the training and testing phases a correlation between the experimental data and results calculated by the neuronal model equal to 0.99 after 337,000 iterations. Figure 6 illustrates the architecture of the proposed neuronal model whose synaptic weights between the different neuron layers and their biases are addressed in Tables 5 to 7.

5.2 Validation of ANN model

As mentioned earlier, validation of the proposed neuronal model after the training and testing phases consists of comparing the results with their application and test data for different soft rock discontinuities.

Figure 7 shows comparisons of the failure envelopes from direct shear test results carried out under CNL conditions presented by Shrivastava & Hao (2017), the results from the proposed ANN model and those ones estimated
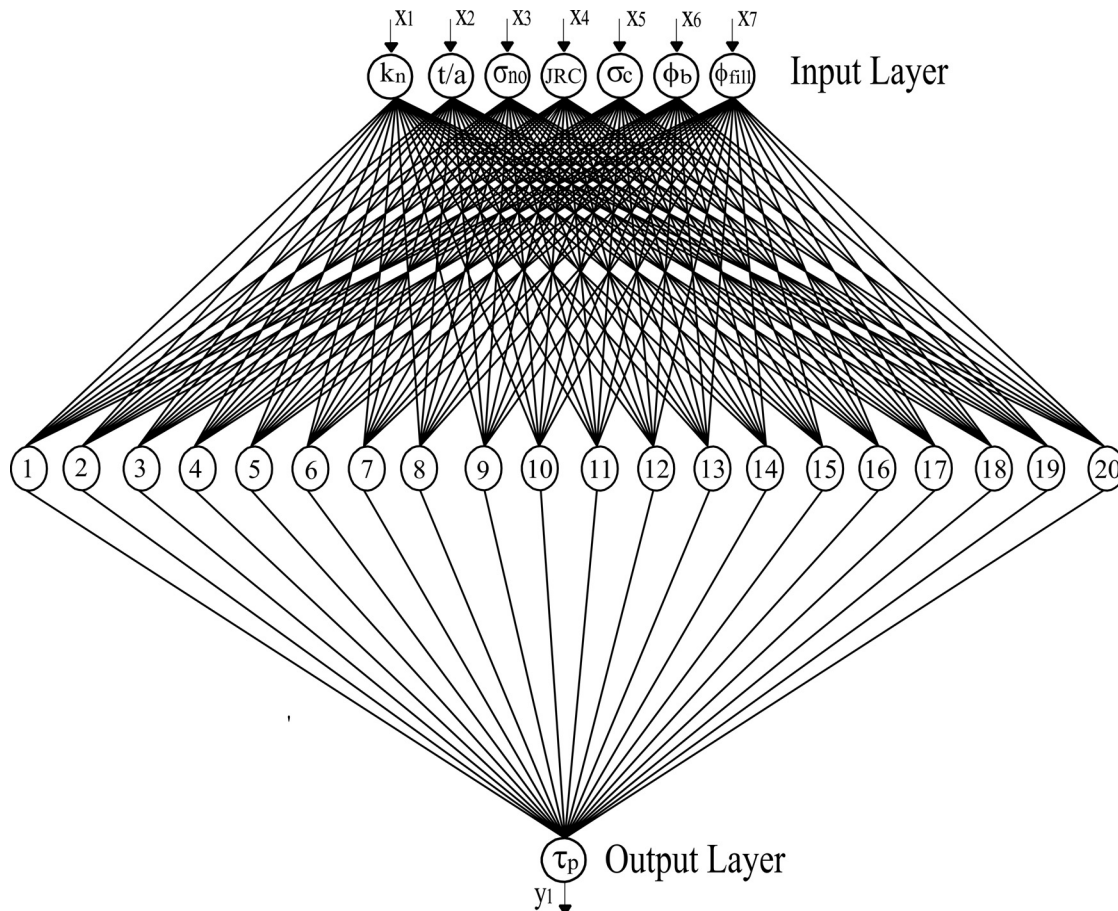

Figure 6. ANN model architecture 7-20-1.

Table 5. Synaptic weights (*wki*) and bias (*bk*) of neurons in hidden layer.

Input	Hidden layer									
	1	2	3	4	5	6	7	8	9	10
x_1	0.1416	-0.8811	0.193	-0.1562	0.0562	-2.3061	-1.9421	3.0309	1.375	0.526
x_2	-0.2145	-0.0837	-0.5042	0.3932	-0.2649	2.3582	-3.7504	-0.8594	0.4828	-0.365
x_3	0.0063	0.16	0.8752	-1.1484	-0.1157	12.786	0.5292	-1.5711	-2.5849	0.1757
x_4	-0.2017	0.7687	-0.3094	0.6241	-0.4964	0.7973	5.2511	-1.2502	0.829	-0.2095
x_5	0.1704	-0.0202	-0.4904	-0.1536	-0.2423	1.6387	-0.2118	0.0581	0.3203	0.0923
x_6	0.2337	-1.1127	0.6014	-0.1615	-0.5537	1.2615	-2.7554	3.2622	0.4041	0.301
x_7	-0.2355	-0.5445	0.6088	-0.0838	-0.5975	3.0077	2.8265	-0.5001	-2.133	0.0831
Bias	0.289	0.4365	0.0379	-0.1559	-0.0911	-1.5388	-0.4761	0.4959	0.7315	0.2195

Table 6. Synaptic weights (*wki*) and bias (*bk*) of neurons in hidden layer (cont.).

Input	Hidden layer									
	11	12	13	14	15	16	17	18	19	20
x_1	-3.2523	-4.881	-0.5783	0.5272	1.5663	0.0281	-0.3282	-0.3803	-3.2965	-2.6106
x_2	-2.3051	-3.6737	5.3678	-0.7055	-1.1681	0.0205	0.2985	0.3775	1.3031	3.7516
x_3	-4.9798	-6.6378	-4.9182	0.899	-0.5241	-0.1658	-0.4961	-0.4149	2.2127	0.3535
x_4	0.9742	0.773	-3.1227	-0.5871	-15.764	0.1729	0.0643	0.7375	4.4023	2.8022
x_5	0.217	-1.6545	3.8664	-0.9088	-1.2279	0.0344	0.3095	0.0699	0.0123	1.0277
x_6	0.9007	2.5998	-0.7639	0.7168	2.54	0.0568	-0.6372	-0.7115	-1.2114	-1.3662
x_7	0.1656	3.262	-0.443	1.2052	-0.427	-0.0958	-0.3801	-0.7264	2.7936	-2.4229
Bias	1.6647	1.2909	4.5642	0.1562	-0.2943	0.1202	0.0439	0.1577	-0.1563	-0.0681

Table 7. Synaptic weights (*wki*) and bias (*bk*) of neurons in output layer.

Output	Hidden layer										
	1	2	3	4	5	6	7	8	9	10	
t	-0.0815	-1.8272	1.0229	-1.3309	-0.6106	5.8633	2.8745	3.363	-3.4452	0.3857	

Output	Hidden layer										
	11	12	13	14	15	16	17	18	19	20	Bias
t	4.1295	-4.2364	-4.5397	1.6681	-7.9778	-0.4047	-1.1373	-1.6871	-4.4917	3.0341	-1.0859

based on the analytical model by Barton and Choubey (1977) for a soft rock discontinuity with σ_c = 11.75 MPa, JRC = 15, ϕ_b = 30° and infill material with ϕ_{fill} = 28.8°. The results show that the neuronal model is able to interpolate the experimental data, and to represent the nonlinear behavior of the failure envelopes as the influence of normal stress and the presence of the infill in the peak shear strength of soft rock discontinuities. Moreover, it more realistically reproduces the shear behavior of the unfilled discontinuity (*t/a* = 0) than the analytical model of Barton & Choubey (1977).

Figure 8 shows the variations in the peak shear strength with the *t/a* ratio for the soft rock discontinuities studied by Haque and Indraratna (2000) under CNS conditions with k_n = 453 kPa/mm, JRC = 4 and 8, σ_c = 12 MPa and ϕ_b = 37.5°, and those obtained by the proposed neuronal model with architecture 7-20-1 for a initial normal stress (σ_{no}) equal to 0.56 MPa, with the infill material of ϕ_{fill} = 35.5°. The results show that the neuronal model once again satisfactorily fit the experimental data and it is also able to express the increase in peak shear strength with the rise in roughness of the discontinuity to low *t/a* ratio values,

and the drop in peak shear strength with the increase in the *t/a* ratio. Similar results were achieved with the neuronal model for soft rock discontinuities and with very low uniaxial compressive strength values (σ_c = 3.5 MPa), JRC = 12, σ_{no} = 0.1 MPa, ϕ_b = 30° and ϕ_{fill} = 30° like those studied by Papaliangas et al. (1993) under CNL conditions, as shown in Figure 9.

Table 8 shows the contribution in percentages of each input variable in the proposed neuronal model's response with architecture 7-20-1 provided by software QNET2000. The results show that within the input vari-

Table 8. Contribution of input variables to the model's response.

k_n	t/a	σ_{n0}	JRC	σ_c	ϕ_b	ϕ_{fill}
6 %	13 %	33 %	20 %	9 %	9 %	10 %

ables considered, the initial normal stress, roughness and *t/a* ratio, that is, the infill, contribute the most in the prediction of the value of the peak shear strength of soft rock discontinuities. Since none of the input variables had a much smaller contribution than the others, the general
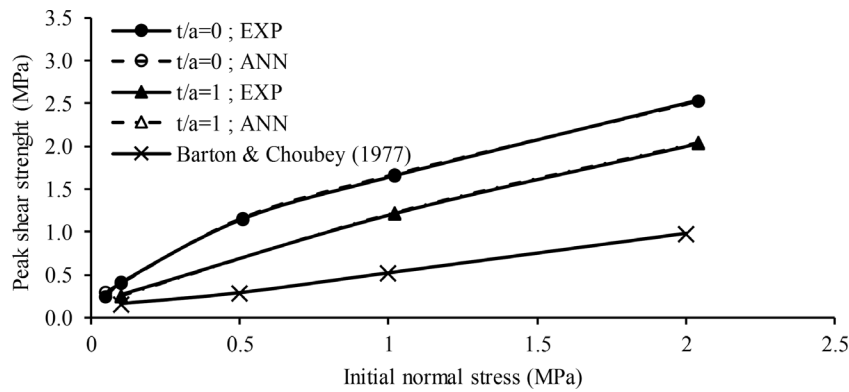

Figure 7. Failure envelopes for soft rock discontinuities from Shrivastava & Hao (2017).
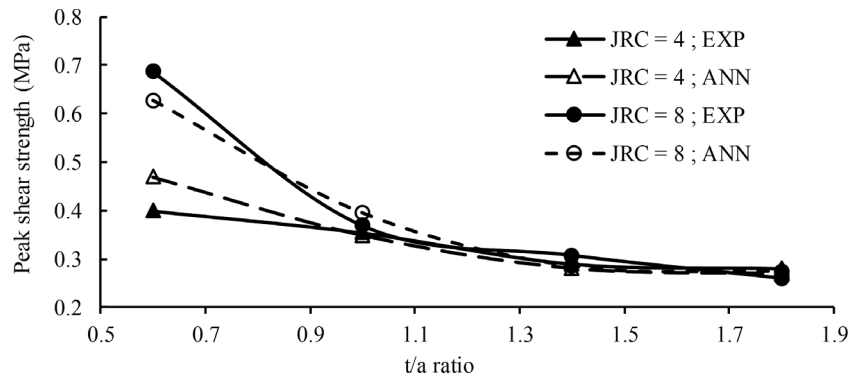

Figure 8. Variation in shear peak strength with the *t/a* ratio for soft rock discontinuities from Haque & Indraratna (2000).
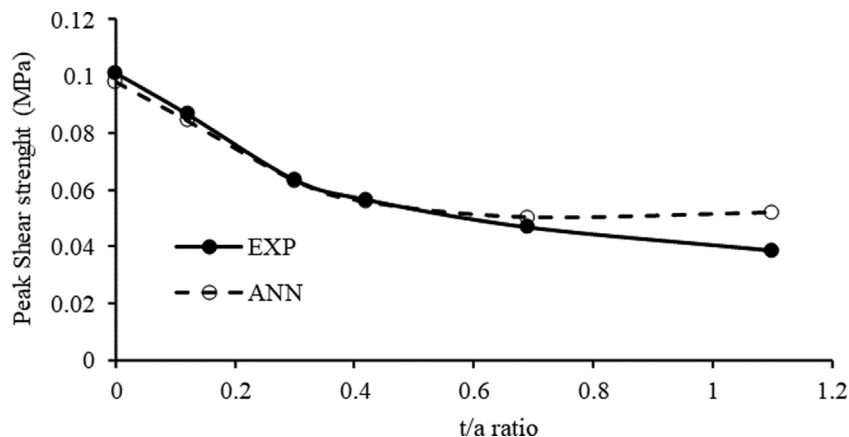

Figure 9. Variation of the shear peak strenght with the *t/a* ratio for very soft rock discontinuities from Papaliangas et al. (1993).

conclusion is that every variable considered in developing the model is relevant regarding the prediction of the peak shear strength of the soft rock discontinuities studied.

5.3 Routine for the use of neuronal model

When developing a neuronal model, the knowledge regarding the phenomenon studied is stored in the values of the synaptic weights and bias obtained after completing the training and testing processes and having made the due validations on the model's behavior. Therefore, knowing about these parameters helps implement the neuronal model in any calculation spreadsheet without requiring specific software, thereby facilitating the use of the predictive model in practical problems in the Rock Mechanics field.

First, after defining the boundary conditions, roughness, intact rock properties and characteristics of the infill material, the input parameters of the rock discontinuity must be normalized using the expression in Equation 20 and the information provided in Table 4. Once the normalized values of the input parameters are in hand, each hidden layer neuron is calculated using the data presented in Tables 5 and 6, and Equations 10-12, adopting the expression in Equations 19 to calculate the output signal of each hidden layer neuron.

Having calculated all hidden layer neurons, their feedforward values calculate the output layer neuron, using the same aforementioned calculation sequence and the synaptic weights and bias in Tables 7 and 8. After using the sigmoid function to calculate the model's response, the peak shear strength of the rock discontinuity in the units system in Table 4 is obtained by transforming the normalized value for the neuron in the output layer also using Equation 20.

The ANN model can be easily used for the representation of constitutive models in numerical analysis. This can be performed using the input variables and the values presented for the synaptic weights and biases in some code to predict the shear behavior of the infilled rock joints.

6. Conclusions

The proposed neuronal model was obtained from 115 large-scale direct shear test results, and the use of 80 % of data available for training and 20 % for validation was efficient, since the proposed neuronal model not only satisfactorily interpolated the test data but was also able to represent the impact of the input variables on the shear strength of soft rock discontinuities, such as, for example, the increase in the peak shear strength with rise in normal stiffness, initial normal stress, roughness and its drop with the increase in the t/a ratio. It is worth mentioning, within the input variables used to develop the proposed neuronal model, the initial normal stress (σ_{no}) and ratio (t/a) as those that most contribute to the model's response.

It is found from the results that the neuronal model that performed best had an architecture 7-20-1, that is, was made up of 7 input variables (normal stiffness, t/a ratio, JRC, uniaxial compressive strength of intact rock in the discontinuity, basic friction angle, and internal friction angle of infill material), 20 neurons in a single hidden layer, the answer being the peak shear strength of soft rock discontinuities. For this model, a correlation was obtained between the calculated and test results of 0.99 after 337,000 iterations in both the training and testing phases.

Since one of the critical characteristics of the artificial neural networks is their capacity to generalize, the proposed neuronal model has diverse application, despite being developed using input data within certain value ranges. Once limitations can be considered only that their application should be restricted to soft rock discontinuities, and should infill material be present, it is of a granular nature, since in the proposed neuronal model the cohesion mechanism was not considered to represent the shear strength of the fill material.

Lastly, it is found that the use of multilayer perceptrons for modelling complex, nonlinear and multivariate phenomena, as in the present case of the shear behavior in soft rock discontinuities it is a valuable tool. Results obtained from the ANN model can be considered satisfactory, even when compared to the use of well-established analytical models. One of its many benefits is the fact that once the training and testing processes are over, and the model duly validated, knowing the architecture of the network, synaptic weights, bias and activation functions of all neurons, it is easy to implement the model in calculation spreadsheets without requiring major computer resources or complex laboratory parameters which availability is still limited.

It is worth emphasizing that the use of artificial neural networks as tools to predict engineering phenomena would not replace any necessary test procedures to determine geotechnical properties of the materials involved in some problem. This tool appears only as an initial additional means to achieve a satisfactory response to a certain problem in order to optimize all the experimental work required.

Acknowledgments

References

Amancio, L.B., Dantas Neto, A.S., & Anjos, G.J.M. (2014). Modelo de previsão de recalques em estacas hélice contínua utilizando redes neurais artificiais. *Proc. XVII Congresso Brasileiro de Mecânica dos Solos e Engenharia Geotécnica, Goiânia*. ABMS, 1-9.

Aydan, Ö., Shimizu, Y., & Kawamoto, T. (1996). The anisotropy of surface morphology characteristics of rock discontinuities. *Rock Mechanics and Rock Engi-*

neering, 29(1), 47-59. https://doi.org/10.1007/BF01019939

Barton, N.R. (1973). A review of a new shear-strength criterion for rock joints. *Engineering Geology*, 7(4), 287-332. https://doi.org/10.1016/0013-7952(73)90013-6

Barton, N.R., & Bandis, S. (1982). Effect of block size on the shear behavior of jointed rock. *Proc. 23rd US Sympium on Rock Mechanics, Berkeley*. ARMA, 739-760.

Barton, N.R., & Bandis, S. (1990). Review of predictive capabilities of JRC-JCS model in engineering practice. *Proc. International Symposium on Rock Joints, Loen*. Balkema, 603-610.

Barton, N.R., & Choubey, V. (1977). The shear strength of rock joints in theory and practice. *Rock Mechanics*, 10(1), 1-54. https://doi.org/10.1007/BF01261801

Benmokrane, B., & Ballivy, G. (1989). Laboratory study of shear behaviour of rock joints under constant normal stiffness conditions. In *Rock Mechanics as a Guide of Efficient Utilization of Natural Resources* (pp. 899-906). Balkema.

Chen, T.C.T., Liu, C.L., & Lin, H.D. (2018). Advanced artificial neural networks. *Algorithms*, 11(7), 102. https://doi.org/10.3390/a11070102

Dantas Neto, S.A., Farias M.M., & Pais, J.C. (2004). Modelagem da viscosidade absoluta dos asfaltos-borracha usando redes neurais artificiais. *Proc. XVIII Congresso da Associação Nacional de Pesquisa e Ensino em Transportes, Florianópolis*. Vol. 8, ANPET, 28-39 (in Portuguese).

Dantas Neto, S.A., Silveira V.S., Amâncio, L.B., & Anjos, G.M. (2014). Pile settlement modeling with multilayer perceptrons. *Electronic Journal of Geotechnical Engineering*, 19, 4517-4528.

Dantas Neto, S.A., Indraratna, B., Oliveira D.A.F., & Assis, P. (2017). Modelling the shear behaviour of clean rock discontinuities using artificial neural networks. *Rock Mechanics and Rock Engineering*, 50(7), 1817-1831. https://doi.org/10.1007/s00603-017-1197-z

Dehghan, S., Sattari, G., Chelgani, C.S., & Aliabadi, M.A. (2010). Prediction of uniaxial compressive strength and modulus of elasticity for travertine samples using regression and artificial neural networks. *Mining Science and Technology*, 20(1), 41-46. https://doi.org/10.1016/S1674-5264(09)60158-7

Farias M.M., Dantas Neto, S.A., & Sousa, R.O. (2003). Prediction of longitudinal roughness using neural network. *Proc. 3rd International Symposium on Maintenance and Rehabilitation of Pavements and Technological Control, Guimarães*. University of Minho, 87-97.

Ghazvinian, A.H., Azinfar, M.J., & Vaneghi, R.G. (2012). Importance of tensile strength on the shear behavior of discontinuities. *Rock Mechanics and Rock Engineering*, 45(3), 349-359. https://doi.org/10.1007/s00603-011-0207-9

Grima M.A., Bruines, P.A., & Verhoef, P.N.W. (2000). Modeling tunnel boring machine performance by neuro-fuzzy methods. *Tunnelling and Underground Space Technology*, 15(3), 259-269. https://doi.org/10.1016/S0886-7798(00)00055-9

Goodman, R.E. (1969). The deformability of joints: Determination of the in-situ modulus of deformation of rock. *Determination Committee D-18 session, Denver*. ASTM, 174-196.

Haque, A. (1999). *Shear behaviour of soft rock joints under constant normal stiffness* [Doctoral dissertation, University of Wollong]. University of Wollong's repository. https://ro.uow.edu.au/theses/1266/

Haque, A., & Indraratna, B. (2000). Experimental and numerical modeling of shear behaviour of rock joints. *Proc. International Conference on Geotechnical & Geological Engineering, Melbourne*. Vol. 1, Lancaster, 1-6.

Haykin, S. (2008). *Neural Networks and Learning Machines*. Pearson.

Horn, H.M., & Deere D.U. (1962). Frictional characteristics of minerals. *Géotechnique*, 12(4), 319-335. https://doi.org/10.1680/geot.1962.12.4.319

Indraratna, B., Haque, A., & Aziz, N. (1999) Shear behaviour of idealized infilled joints under constant normal stiffness. *Géotechnique*, 49(3), 331-355. https://doi.org/10.1680/geot.1999.49.3.331

Indraratna, B., Welideniya, H.S., & Brown, E.T. (2005). A shear strength model for idealized infilled joints under constant normal stiffness. *Géotechnique*, 55(3), 215-226. https://doi.org/10.1680/geot.2005.55.3.215

Indraratna, B., Jayanathan, M., & Brown, E.T. (2008a). Shear strength model for overconsolidated clay-infilled idealised rock joints. *Géotechnique*, 58(1), 55-65. https://doi.org/10.1680/geot.2008.58.1.55

Indraratna, B., Oliveira D.A.F., & Jayanathan, M. (2008b). Revised shear strength model for infilled rock joints considering overconsolidation effect. *Proc. 1st Southern Hemisphere International Rock Mechanics Symposium, Perth*. ACG, 16-19.

Indraratna, B., Oliveira, D.A.F., & Brown, E.T. (2010). A shear-displacement criterion for soil-infilled rock discontinuities. *Géotechnique*, 60(8), 623-633. https://doi.org/10.1680/geot.8.P.094

Indraratna, B., Fasce, A.M., Oliveira, D.A.F., & Premadasa, W. (2012). Shear behaviour of rock joints under cyclic loading. *Proc. 11th Australia - New Zealand Conference on Geomechanics: Ground Engineering in a Changing World, Melbourne*. AGS & NZGS, 1256-1261.

Indraratna, B., Premadasa, W., & Brown, E.T. (2013). Shear behaviour of rock joints with unsaturated infill. *Géotechnique*, 63(15), 1356-1360. https://doi.org/10.1680/geot.12.P.065

Indraratna, B., Premadasa, W., Brown, E.T., Gens, A., & Heitor, A. (2014). Shear strength of rock joints influ-

enced by compacted infill. *International Journal of Rock Mechanics and Mining Sciences*, 70, 296-307. https://doi.org/10.1016/j.ijrmms.2014.04.019

Indraratna, B., Kumara, C., Zhu, S-P., & Sloan, S. (2015). Mathematical modeling and experimental verification of fluid flow through deformable rough rock joints. *International Journal of Geomechanics*, 15(4), 04014065. https://doi.org/10.1061/(ASCE)GM.1943-5622.0000413

Jang, H.S., & Jang, B.A. (2015). New method for shear strength determination of unfilled, unweathered rock joint. *Rock Mechanics and Rock Engineering*, 48(4), 1515-1534. https://doi.org/10.1007/s00603-014-0660-3

Karakus, M., Liu, Y., Zhang, G., & Tang, H. (2016). A new shear strength model incorporating influence of infill materials for rock joints. *Geomechanics and Geophysics for Geo-Energy and Geo-Resources*, 2(3), 183-193. https://doi.org/10.1007/s40948-016-0032-4

Kumar, R., & Verma, A.K. (2016). Anisotropic shear behavior of rock joint replicas. *International Journal of Rock Mechanics and Mining Sciences*, 90, 62-73. https://doi.org/10.1016/j.ijrmms.2016.10.005

Ladanyi, B., & Archambault, G. (1977). Shear strength and deformability of filled indented joints. In: Proc. *International Symposium on Geotechnics of Structurally Complex Formations.* Vol. 1, AGI, 317-326.

Lee, Y-K., Park, J-W., & Song, J-J. (2014). Model for the shear behavior of rock joints under CNL and CNS Conditions. *International Journal of Rock Mechanics and Mining Sciences*, 70, 252-263. https://doi.org/10.1016/j.ijrmms.2014.05.005

Leite, A.R.S., Dantas Neto, S.A., Polemis Júnior, K., & Oliveira, C.M.O. (2019). Study on the shear behaviour of rock joints using different models of artificial neural networks. *Proc. International Congress on Rock Mechanics and Rock Engineering*, *Foz do Iguaçu*. Vol. 6. CRC Press, 2707-2714.

Matos, Y.M.P. (2018). *Development of models of prediction of the shear behavior in discontinuities without filling of rock masses using fuzzy and neuro-fuzzy techniques* [Master's dissertation, Federal University of Ceará]. Federal University of Ceará's repository. http://www.repositorio.ufc.br/handle/riufc/30223

Matos, Y.M.P., Dantas Neto, S.A., & Barreto, G.A. (2019a). A Takagi-Sugeno fuzzy model for predicting the clean rock joints shear strength. *REM - International Engineering Journal*, 72(2), 193-198. https://doi.org/10.1590/0370-44672018720083

Matos, Y.M.P., Dantas Neto, S.A., & Barreto, G.A. (2019b). Predicting the shear strength of unfilled rock joints with the first-order Takagi-Sugeno fuzzy approach. *Soils and Rocks*, 42(1), 21-29. https://doi.org/10.28927/SR.421021

Mehrishal, S., Sharifzadeh, M., Shahriar, K., & Song, J.J. (2016). An experimental study on normal stress and shear rate dependency of basic friction coefficient in dry and wet limestone joints. *Rock Mechanics and Rock Engineering*, 49(12), 4607-4629. https://doi.org/10.1007/s00603-016-1073-2

Moshrefii, S., Shahriar, K., Ramezanzadeh, A., & Goshtasbi, K. (2018). Prediction of ultimate strength of shale using artificial neural network. *Journal of Mining and Environment*, 9(1), 91-105. https://doi.org/10.22044/jme.2017.5790.1390

Naghadehi, M.Z. (2015). Laboratory study of the shear behaviour of natural rough rock joints infilled by different soils. *Periodica Polytechnica Civil Engineering*, 59(3), 413-421. https://doi.org/10.3311/PPci.7928

Oliveira, D.A.F., Indraratna, B., & Nemcik, J. (2009). Critical review on shear strength models for soil-infilled joints. *Geomechanics and Geoengineering*, 4(3), 237-244. https://doi.org/10.1080/17486020903128564

Papaliangas, T., Lumsden, A.C., Hencher, S.R., & Manolopoulou, S. (1990). Shear strength of modelled filled rock joints. *Proc. International Symposium on Rock Joints*, *Loen*. Balkema, 275-282.

Papaliangas, T., Hencher, S.R., Lumsden, A.C., & Manolopoulou, S. (1993). The effect of frictional fill thickness on the shear strength of rock discontinuities. *International Journal of Rock Mechanics and Mining Sciences and Geomatics*, 30(2), 81-91. https://doi.org/10.1016/0148-9062(93)90702-F

Patton, F.D. (1966). Multiple modes of shear failure in rocks. *Proc. 1st Congress of the International Society for Rock Mechanics*, *Lisbon*. Vol. 1, LNEC, 509-513.

Premadasa, W., & Indraratna. (2015). Shear behaviour of infilled rock joints related to partially saturated infill conditions. *Proc. International Conference on Geotechnical Engineering, Colombo*. SLGS, 1-4.

Richard, L.R. (1975). *The shear strength of joints in weathered rock* [Doctoral dissertation, University of London]. University of London's repository. http://hdl.handle.net/10044/1/22541

Rumelhart, D.E., Hinton, G.E., & Williams, R.J. (1986). Learning representations by back-propagating errors. *Nature*, 323, 533-536. https://doi.org/10.1038/323533a0

Runxuan, Z. (2006). *Efficient sequential and batch learning artificial neural network methods for classification problems* [Doctoral dissertation, Nanyang Technological University]. Nanyang Technological University's repository. https://doi.org/10.32657/10356/3468

Schmidhuber, J. (2015). Deep learning in neural networks: An overview. *Neural Networks*, 61, 85-117. https://doi.org/10.1016/j.neunet.2014.09.003

Shrivastava, A.K., & Rao, K.S. (2017). Physical modeling of shear behavior of infilled rock joints under CNL and CNS boundary conditions. *Rock Mechanics and Rock Engineering*, 51(1), 101-118. https://doi.org/10.1007/s00603-017-1318-8

Singh, V.K., Singh, D., & Singha, T.N. (2001). Prediction of strength properties of some schistose rocks from

petrographic properties using artificial neural networks. *International Journal of Rock Mechanics and Mining Sciences*, 38(2), 269-284. https://doi.org/10.1016/S1365-1609(00)00078-2

Singh, H.K., & Basu, A.A. (2018). Comparison between the shear behavior of `real' natural rock discontinuities and their replicas. *Rock Mechanics and Rock Engineering*, 51(1), 329-340. https://doi.org/10.1007/s00603-017-1334-8

Skinas, C.A., Bandis, S.C., & Demiris, C.A. (1990). Experimental Investigations and Modelling of Rock Joint Behaviour Under Constant Stiffness. *Proc. International Symposium on Rock Joints*. Balkema, 301-307.

Sonmez, H., Ercanoglu, M., Kalender, A., Dagdelenler, G., & Tunusluogly, R. (2016). Predicting uniaxial compressive strength and deformation modulus of volcanic bimrocks considering engineering dimension. *International Journal of Rock Mechanics and Mining Sciences*, 86, 91-103. https://doi.org/10.1016/j.ijrmms.2016.03.022

Tang, Z.C., Liu, Q.S., & Huang, J.H. (2014). New criterion for rock joints based on three- dimensional roughness parameters. *Journal of Central South University*, 21(12), 4653-4659. https://doi.org/10.1007/s11771-014-2473-7

Tatone, B.S., & Grasselli, G. (2009). A method to evaluate the three-dimensional roughness of fracture surfaces in brittle geomaterials. *Review of Scientific Instruments*, 80(12), 1-10. https://doi.org/10.1063/1.3266964

Xia, C.C., Tang, Z.C., Xiao, W.M., & Song, Y.L. (2014). New peak shear strength criterion of rock joints based on quantified surface description. *Rock Mechanics and Rock Engineering*, 47(2), 387-400. https://doi.org/10.1007/s00603-013-0395-6

Yang, J., Rong, G., Cheng, L., Hou, D., & Wang, X. (2016). Experimental study of peak shear strength of rock joints. *Chinese Journal of Rock Mechanics and Engineering*, 34(5), 884-894. https://doi.org./10.13722/j.cnki.jrme.2014.1096-en

Yilmaz, I., & Yuksek, A.G. (2008). An example of artificial neural network (ANN) application for indirect estimation of rock parameters. *Rock Mechanics and Rock Engineering*, 41(5), 781-795. https://doi.org/10.1007/s00603-007-0138-7

Zeigler, T.W. (1972). In situ tests for the determination of rock mass shear strength - Technical Report S-72-12. *US Army Engineer Waterways Experiment Station, Vicksburg, MS*.

Zhang, X., Jiang, Q., Chen, N., Wei, W., & Feng, X. (2016). Laboratory investigation on shear behavior of rock joints and a new peak shear strength criterion. *Rock Mechanics and Rock Engineering*, 49(9), 3495-3512. https://doi.org/10.1007/s00603-016-1012-2